ARTICLES

*Journal of Semiconductors*
(2019) 40, 122802
doi: 10.1088/1674-4926/40/12/122802

# A contrivance of 277 nm DUV LD with $B_{0.313}Ga_{0.687}N/B_{0.40}Ga_{0.60}N$ QWs and $Al_xGa_{1-x}N$ heterojunction grown on AlN substrate

**Mussaab I. Niass[1, 2, 3, †], Muhammad Nawaz Sharif[1, 2, 3], Yifu Wang[1, 2, 3], Zhengqian Lu[1, 2, 3], Xue Chen[1, 2, 3], Yipu Qu[1, 2, 3], Zhongqiu Du[1, 2, 3], Fang Wang[1, 2, 3, †], and Yuhuai Liu[1, 2, 3, †]**

[1]National Center for International Joint Research of Electronic Materials and Systems, Zhengzhou 450001, China

[2]International Joint-Laboratory of Electronic Materials and Systems of Henan Province, Zhengzhou 450001, China

[3]Department of Electronics and Information Engineering, School of Information Engineering, Zhengzhou University, Zhengzhou 450001, China

**Abstract:** In this paper, an ultraviolet C-band laser diode lasing at 277 nm composed of $B_{0.313}Ga_{0.687}N/B_{0.40}Ga_{0.60}N$ QW/QB heterostructure on Mg and Si-doped $Al_xGa_{1-x}N$ layers was designed, as well as a lowest reported substitutional accepter and donor concentration up to $N_A = 5.0 \times 10^{17}$ cm$^{-3}$ and $N_D = 9.0 \times 10^{16}$ cm$^{-3}$ for deep ultraviolet lasing was achieved. The structure was assumed to be grown over bulk AlN substrate and operate under a continuous wave at room temperature. Although there is an emphasizing of the suitability for using boron nitride wide band gap in the deep ultraviolet region, there is still a shortage of investigation about the ternary BGaN in aluminum-rich AlGaN alloys. Based on the simulation, an average local gain in quantum wells of 1946 cm$^{-1}$, the maximum emitted power of 2.4 W, the threshold current of 500 mA, a slope efficiency of 1.91 W/A as well as an average DC resistance for the *V–I* curve of (0.336 Ω) had been observed. Along with an investigation regarding different EBL, designs were included with tapered and inverse tapered structure. Therefore, it had been found a good agreement with the published results for tapered EBL design, with an overweighting for a proposed inverse tapered EBL design.

**Key words:** laser diodes; semiconducting aluminum compounds; heterojunction semiconductor devices; quantum wells; semiconducting ternary compounds

**Citation:** M I Niass, M N Sharif, Y F Wang, Z Q Lu, X Chen, Y P Qu, Z Q Du, F Wang, and Y H Liu, A contrivance of 277 nm DUV LD with $B_{0.313}Ga_{0.687}N/B_{0.40}Ga_{0.60}N$ QWs and $Al_xGa_{1-x}N$ heterojunction grown on AlN substrate[J]. *J. Semicond.*, 2019, 40(12), 122802. http://doi.org/10.1088/1674-4926/40/12/122802

## 1. Introduction

Vast promising applications for deep ultraviolet laser diode (DUVLD) in many fields such as wireless communication, medical instruments and chemical devices are still waiting for the higher performance of laser diode (LD) to be achieved[1, 2]. Thus, one of the core obstacles yet to be overcome is the p-type conductivity mainly due to the higher activation energy of Mg-dopant[3] for higher Al composition, which probably causes an increase in resistivity.

Many studies have shown and demonstrated that the potential for exploiting h-BN in far-ultraviolet (FUV) emitters are due to its good characteristics[4, 5]. Also, the ternary BGaN and quaternary BAlGaN are found to be suitable for growing over (0001) 6H-SiC by MOVPE[6]. Although $B_{0.01}Ga_{0.99}N/Al_{0.12}Ga_{0.88}N$ MQWs LED had been successfully grown over 6H-SiC with a PL peak at 360 nm[7, 8], Mg-doped h-BN used as a contact and electron blocking layer (EBL) layer instead of p-AlN is successfully studied in Al-rich AlGaN LED[9–11]. However, there is no laser diode (LD) structure simulation that investigated $B_xGa_{1-x}N/Al_xGa_{1-x}N$ in deep ultraviolet (DUV). Therefore, this paper seeks to demonstrate a new LD structure that exhibits the potential of using wurtzite trinity $B_{0.313}GaN/B_{0.40}GaN$ and AlGaN assumed to be grown over AlN substrate without any conventional contact layer.

Correspondence to: M I Niass, mussaab99@gmail.com; F Wang, iefwang@zzu.edu.cn; Y H Liu, ieyhliu@zzu.edu.cn

Received 26 DECEMBER 2018; Revised 30 APRIL 2019.



## 2. Simulation model

The simulated laser diode structure was conducted via using LASTIP-Crosslight simulator software with a self-consistency model for varies quantity calculations. Were mirror reflectivity factors of (0.05) for both facets were assumed and a cavity length of 1500 $\mu$m. The spacer-1 and spacer-2 layers in the Table 1 were proposed for reducing the band-offset between AlGaN and BGaN layers.

## 3. Results and discussions

According to simulation results, it has been found that the minimum doping concentration that exhibits lasing at 277 nm for the given structure is $N_A = 5 \times 10^{17}$ cm$^{-3}$, $N_D = 9 \times 10^{16}$ cm$^{-3}$ with an OCF of 40.4 % as shown in Fig. 1. Therefore, different EBL design has been studied, firstly the conventional EBL contrivance which have a constant composition along the layer thickness assumed to be 10 nm, as well as an aluminum content of 80% ($Al_{0.8}GaN$), were adjusted.

Therefore, barely the structure produces an emission for $P_{max} = 115$ $\mu$W given at a maximum current injection of $I_m = 550$ mA and $I_{th} = 150$ mA as shown in Fig. 2. Whereas the *V–I* characteristic curve shows a semi-linear relationship for an approximated (biasing voltage) $V_{th} = 7$ V, with a DC resistance of 0.77 Ω.

Secondly, for the tapered (linearly graded) EBL contriv-

Table 1. The contrived LD structure at room temperature for $B_{0.313}GaN/B_{0.40}GaN$ MQW (p, p-type Mg-dopant; n, n-type Si-dopant; i, intrinsic/no-doping; CLL, cladding layer; WG, wave guide; EBL-IT, electron blocking layer-inverse tapered).

| Layer material | Layer function | Thickness (nm) | Real refractive index |
|---|---|---|---|
| p-$Al_{0.87}GaN$ | p-WG | 500 | 2.20 |
| p-$Al_{0.71–0.77}GaN$ | p-CLL | 150 | 2.263–2.239 |
| i-$Al_{0.80–0.65}GaN$ | EBL-IT | 10 | 2.228–2.286 |
| p-$Al_{0.57}GaN$ | Spacer-1 | 10 | 2.317 |
| i-$B_{0.40}GaN \times (3)$ | QB | 5 | 2.343 |
| i-$B_{0.313}GaN \times (2)$ | QW | 4 | 2.286 |
| n-$Al_{0.61–0.58}GaN$ | Spacer-2 | 10 | 2.30–2.313 |
| n-$Al_{0.77–0.71}GaN$ | n-CLL | 100 | 2.24–2.63 |
| n-$Al_{0.77}GaN$ | n-WG-1 | 685 | 2.24 |
| n-$Al_{0.77}GaN$ | n-WG-2 | 1800 | 2.24 |
| i-AlN | Substrate | 2000 | 2.15 |

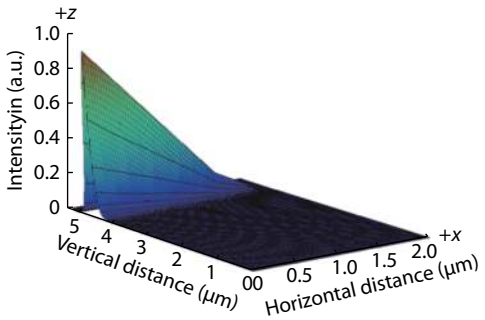


Fig. 1. (Color online) The optical intensity confined within the active region for optical confining factor (OCF) of 40.4%.

ance a composition of $Al_{0.65–0.80}GaN$ was adjusted. Thus, the following quantities had been calculated by the simulator, were $P_{max}$ = 1.73 W at $I_{max}$ = 1.65 A observed in Fig. 2 as well as $I_{th}$ = 600 mA, S.E. = 1.468 W/A, $V_{th}$ = 5 V, $R$ = 0.239 Ω.

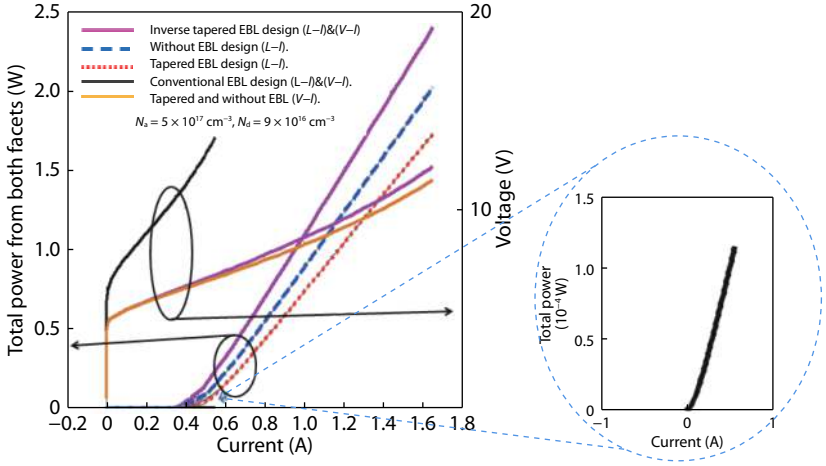


Fig. 2. (Color online) Illustrate the *L–I* and *V–I* electrical characteristic curves for the conventional EBL, tapered EBL, without EBL and inverse tapered EBL designs.

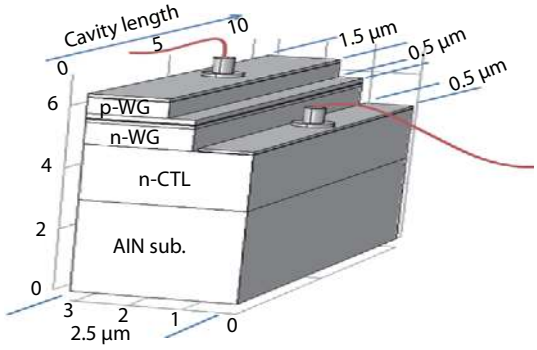


Fig. 3. (Color online) Schematic illustrations for the right half of simulated structure, real cavity length are 1500 $\mu$m.

Thirdly, when a removal of EBL layer was established it shows an enhances in *S.E.* and threshold current almost by 15.8% and 8.3% achieved respectively, comparing to tapered design. Hence $P_{max}$ = 2.02 W at $I_{max}$ = 1.65 A, $I_{th}$ = 550 mA and S.E. = 1.70 W/A. On the other side, *V–I* curve shows a biasing voltage $V_{th}$ = 5 V, $R$ = 0.262 Ω, the lowest resistance is obvious since there is no EBL layer. Lastly, for an inverse tapered EBL contrivance as shown in Table 1 and in Fig. 3. gives $P_{max}$ = 2.4 W, $I_{max}$ = 1.65 A, $I_{th}$ = 500 mA and S.E. = 1.91 W/A a very good enhances were achieved in S.E. and $I_{th}$ by 12.3% and 9% respectively, in addition to same tapered design threshold voltage was observed but different resistance of 0.336 Ω. Therefore, these results in well agree with published results at Ref. [12] in term of a better performance could be obtained, if tapered EBL design is applied instead of conventional EBL. Therefore this paper demonstrated an alternative opportunity of having higher performance for LD by using inverse tapered EBL design over tapered and conventional EBL.

Since the conventional EBL structure exhibits a very low emission power compared to other designs, probably due to low doping concentrations. Hence, we applied an increase in the doping concentration magnitude order, thus it had been found that an increase in $N_A$ and $N_D$ by two orders of magnitude up to $N_A = 5 \times 10^{20}$ cm$^{-3}$, $N_D = 9 \times 10^{19}$ cm$^{-3}$ lead to a clear stimulated emission in the conventional structure. Therefore, the simulated results for those concentrations shows same *L–I* and *V–I* characteristic curves for tapered, inverse tapered and without EBL designs, were $P_{max}$ = 103.8 W at $I_{max}$ = 51.5 A, $I_{th}$ = 500 mA, S.E. = 2.0 W/A, $V_{th}$ = 4.6 V and $R$ = 0.144 Ω as shown in Figs. 4(a) and 4(b). While the conventional structure shows enhance in the S.E. (3.14 W/A) by 57% compared to the other three designs in this high accepter and

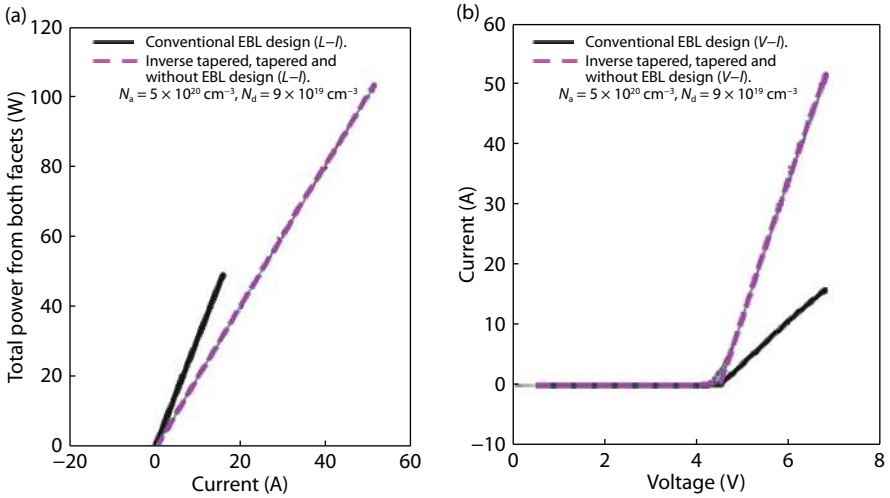


Fig. 4. (Color online) Showing the (a) *L*–*I* and (b) *V*–*I* curve for the two LD structure for the conventional EBL, tapered EBL, without EBL and inverse tapered EBL designs with the $N_A = 5 \times 10^{20}$ cm$^{-3}$, $N_D = 9 \times 10^{19}$ cm$^{-3}$.

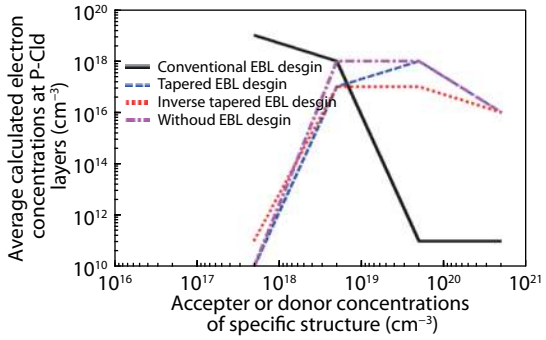


Fig. 5. (Color online) Showing the relationship between the averages calculated electron concentrations within the P-Cladding layer for different accepter and donor concentrations for the four EBL designs.

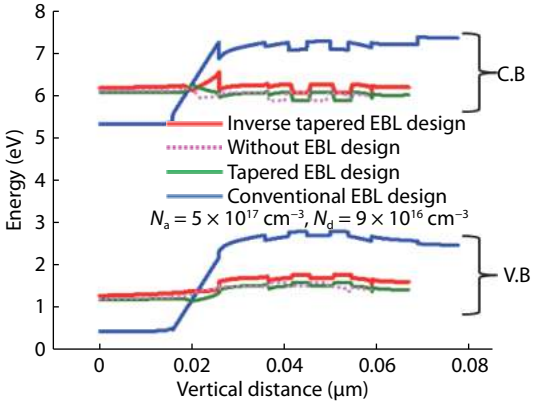


Fig. 6. (Color online) Vertical cut view for the LD structure that illustrates the band diagram for the active region and EBL layer, with the $N_A = 5 \times 10^{17}$ cm$^{-3}$, $N_D = 9 \times 10^{16}$ cm$^{-3}$ for the four different EBL layers.

donor concentrations. Were $P_{max}$ = 50 W at $I_{max}$ = 15.9 A, $I_{th}$ = 130 mA $V_{th}$ = 4.8 V, although a very good enhancement in S.E. is shown by the conventional design a higher resistance of 0.563 Ω compared to previously mentioned resistance for the other structures. In addition to a limitation in the maximum emitted power by almost 51% is observed, these limitations probably due to: (1) The electron leakage into the p-cladding layers, as shown in Fig. 5. (2) The band-offset height that forms as a result of EBL composition difference between the QB/Spacer-2, directly coupled to the resistance.

It has been found that the electron concentrations within the quantum well for the three designs (tapered, inverse tapered and without EBL) almost $10^{19}$–$10^{20}$ cm$^{-3}$. While the conventional EBL contrivance found to be $10^{18}$–$10^{19}$ cm$^{-3}$ which means lower concentration by one order of magnitude from the sufficient concentrations, therefore it is the probable reason for why there is no an apparent stimulated emission for the conventional structure, shown in Fig. 2 especially for lower accepter and donor concentrations.

For more elaboration of the first reason regarding the leakage of current/electrons, an analysis for the electron concentration in the p-cladding layer is summarized for the four different doping concentrations as shown in Fig. 5. Thus, it found that for a concentration of $N_A = 5 \times 10^{17}$ cm$^{-3}$, $N_D = 9 \times 10^{16}$ cm$^{-3}$ the three designed structures show a low concentration of $10^{10}$ cm$^{-3}$. While a larger amount of leakage current found for the conventional design ~ $10^{19}$ cm$^{-3}$ almost similar quantity of electrons found in QW, that may mean there is no blocking happened for the electrons as could be observed from Fig. 6. This larger amount of leakage electron it has been evident to be due to insufficient EBL barrier/offset. While an attempt to increase the EBL composition for the given $N_A$ and $N_D$ concentrations seems to increase the $V_{th}$.

In addition to that, it will lead to a reverse increase of EBL height in the valence band, thus forming an undesired hole blocking layer that may directly degrade the p-type conductivity. On the other side, a tendency to increase the doping concentrations around $10^{19}$ cm$^{-3}$ gives p-cladding layer concentration approximately to $10^{17}$ cm$^{-3}$ for the three structures and $10^{11}$ cm$^{-3}$ for a conventional design. These higher theoretical $N_A$ and $N_D$ i.e. > $10^{18}$ cm$^{-3}$ it might be difficult to implements practically, while $N_A$ and $N_D$ < $10^{17}$ cm$^{-3}$ have a higher possibility to be implemented for the demonstrated aluminum content.

## 4. Conclusion

The contrivances of a new combination between BGaN and AlGaN alloys were proposed, for $B_{0.313}GaN/B_{0.4}GaN$ quantum well/quantum barrier assumed to be grown over AlN substrate. Hence a lasing in a deep ultraviolet range in 277 nm

were observed, with a maximum emitted power of 2.4 W at an injection current of 1.65 A, threshold current of 500 mA and slope efficiency of 1.91 W/A that represents 9 %, 12.3% enhancement compared to tapered design respectively. With the lowest reported accepter and donor concentration for DUV devices of $N_A = 5 \times 10^{17}$ cm$^{-3}$, $N_D = 9 \times 10^{16}$ cm$^{-3}$.

In addition to an investigation regarding different EBL designs were shown. Therefore, we found it agreed well with the published results, moreover this paper proposes a probable better EBL design, especially for low doping concentrations, called inverse tapered EBL.

## Acknowledgement

This work is provisioned by National Key Research and Development Program (Nos. NKRDP 2016YFE0118400), the Key project of Science and Technology of Henan Province (No. 172102410062), National Natural Science Foundation of China (No. 61176008), and National Natural Science Foundation of China Henan Provincial Joint Fund Key Project (No. U1604263).

### Appendix A

Table A1. BN, GaN and AlN wurtzite parameters.

| Parameter | BN[13] | GaN** | AlN** |
|---|---|---|---|
| Energy gap (eV) | 6.20 | 3.42 | 6.20 |
| Ref_Affinity (eV) | 4.5 | 4.0 | 4.07 |
| Lattice const. (Å) | 3.6157 | 3.189 | 3.112 |
| Spin-orbit splitting* | $\Delta_1 = \Delta_{Cr} = 0.016$ | $\Delta_1 = \Delta_{Cr} = 0.042$ | $\Delta_1 = \Delta_{Cr} = 0.0585$ |
| Crystal-field splitting (eV)* | $\Delta_2 = \Delta_3 = \frac{\Delta_{So}}{3} = 0.001$ | $\Delta_2 = \Delta_3 = \frac{\Delta_{So}}{3} = 0.0043$ | $\Delta_2 = \Delta_3 = \frac{\Delta_{So}}{3} = 0.0068$ |
| Effective electron mass ($m_0$) | $m_{e\|\|} = 0.35$, $m_{e\perp} = 0.24$ | $m_{e\|\|} = 0.20$, $m_{e\perp} = 0.18$ | $m_{e\|\|} = 0.33$, $m_{e\perp} = 0.25$ |
| Valance-band effective-mass parameter ($\frac{\hbar^2}{2m}$) | $A_1 = -4.667$, $A_2 = -1.0$, $A_3 = 3.667$, $A_4 = -1.8355$, $A_5 = -1.079$, $A_6 = -0.46$ | $A_1 = -7.24$, $A_2 = -0.51$, $A_3 = 6.73$, $A_4 = -3.36$, $A_5 = -3.35$, $A_6 = -4.72$ | $A_1 = -3.95$, $A_2 = -0.27$, $A_3 = 3.68$, $A_4 = -1.84$, $A_5 = -1.95$, $A_6 = -2.91$ |
| Deformation potential (interband) (eV) | $a = -8.16$, $a_c = a/2 = -4.08$ | $a = -8.16$, $a_c = a/2 = -4.08$ | $a = -8.16$, $a_c = a/2 = -4.08$ |
| Elastic stiffness constant ($10^{11}$ dyn/cm$^2$ | $C_{33} = 7.38$, $C_{13} = 4.69$ | $C_{33} = 39.2$, $C_{13} = 10.0$ | $C_{33} = 39.5$, $C_{13} = 12.0$ |
| Deformation potential (eV)* | $D_1 = 0.7$, $D_2 = 2.1$, $D_3 = 1.4$, $D_4 = -0.7$ | $D_1 = -0.89$, $D_2 = 4.27$, $D_3 = 5.18$, $D_4 = -2.59$ | $D_1 = 0.7$, $D_2 = 2.1$, $D_3 = 1.4$, $D_4 = -0.7$ |

*The deformation potential for BN assumed to have the same quantities of GaN, and since the spin-orbit, crystal-field splitting's of BN given in Ref. [13] and due to a programming issue they have been approximated to the given values. ** Available at simulator macros.

## References

[1] Li D B, Sun X J, Guo C L. AlGaN photonics: recent advances in materials and ultraviolet devices. Adv Opt Photon, 2018, 10, 43

[2] Chowdhury M Z, Hossan M T, Islam A, et al. A comparative survey of optical wireless technologies: architectures and applications. IEEE Access, 2018, 6, 9819

[3] Chen J R, Ko T S, Su P Y, et al. Numerical study on optimization of active layer structures for GaN/AlGaN multiple-quantum-well laser diodes. J Lightwave Technol, 2008, 26, 3155

[4] Watanabe T, Niiyama T, Miya K, et al. Far-ultraviolet plane-emission handheld device based on hexagonal boron nitride. Nat Photonics, 2009, 3, 591

[5] Watanabe K, Taniguchi T. Hexagonal boron nitride as a new ultraviolet luminescent material and its application. Int J Appl Ceram Technol, 2011, 8, 977

[6] Kawanishi H, Haruyama M, Shirai T, et al. (BAlGa)N quaternary system and epitaxial growth on (0001) 6H-SiC substrate by low-pressure MO-VPE. Proc SPIE, 1997, 2994, 52

[7] Kurimoto M, Takano T, Yamamoto J, et al. Growth of BGaN/AlGaN multi-quantum-well structure by metalorganic vapor phase epitaxy. J Cryst Growth, 2000, 221, 378

[8] Honda T, Kurimoto M, Shibata M, et al. Excitonic emission of BGaN grown on (0 0 0 1) 6H-SiC by metal-organic vapor-phase epitaxy. J Lumin, 2000, 87–89, 1274

[9] Dahal J L R, Majety S, Pantha B N, et al. Epitaxially grown semiconducting hexagonal boron nitride as a deep ultraviolet photonic materia. Appl Phys Lett, 2011, 98, 211110

[10] Majety J L S, Cao X K, Dahal R, et al. Epitaxial growth and demonstration of hexagonal BN/AlGaN p–n junctions for deep ultraviolet photonics. Appl Phys Lett, 2012, 100, 061121

[11] Jiang H X, Lin J Y. Hexagonal boron nitride for deep ultraviolet photonic devices. Semicond Sci Technol, 2014, 29, 1

[12] Satter M M, Kim H J, Lochner Z, et al. Design and analysis of 250-nm AlInN laser diodes on AlN substrates using tapered electron blocking layers. IEEE J Quantum Electron, 2012, 48, 703

[13] Sailo L, Ralte R L, Lalchhuanawmi M, et al. Calculation of the band structure and band splitting energy of boron compounds (BX, X = N, P, As, Sb) using modified Becke-Johnson potential. IOSR-JAP, 2016, 8, 1